Catalytic Conversion of Graphene into Carbon Nanotubes *via* Gold Nanoclusters at Low Temperatures

Enkeleda Dervishi,*,† Shawn Bourdo,† Joshua A. Driver,† Fumiya Watanabe,† Alexandru R. Biris,‡ Anindya Ghosh,§ Brian Berry,§ Viney Saini,† and Alexandru S. Biris*,†

†Nanotechnology Center, University of Arkansas at Little Rock, Little Rock, Arkansas 72204, United States , ‡National Institute for Research and Development of Isotopic and Molecular Technologies, Cluj-Napoca, Romania, and §Chemistry Department, University of Arkansas at Little Rock, Little Rock, Arkansas 72204, United States

ABSTRACT

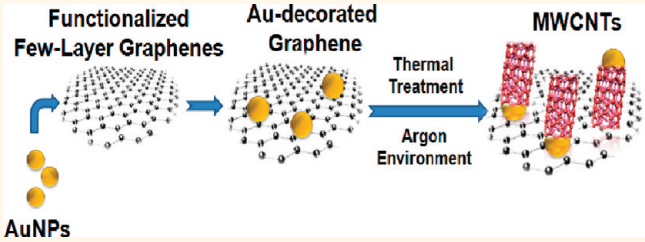

Here, we present the catalytic conversion of graphene layers into carbon nanotubes (CNTs), in the presence of Au nanoparticles (AuNPs) without the need for an additional carbon source. We have demonstrated that this catalytic process takes place at temperatures as low as 500 °C. No other oxide supports decorated with AuNPs were found to grow CNTs at this temperature. These findings highlight the high activity of graphene when used as a support for catalytic reactions.

KEYWORDS: graphene · gold nanoparticles · carbon nanotubes · chemical vapor deposition · radio frequency heating/excitation

Since their discovery, CNTs and graphene have been the most intensively researched carbon allotropes,[1,2] due to their exceptional thermal, optical, electronic, and mechanical properties.[3,4] These graphitic nanomaterials have been proposed as the foundation for various transformative technologies ranging from energy harvesting,[5] multifunctional composites and sensors,[6] to nanomedicine.[7] The development of multicomponent composite systems based on such carbon nanomaterials, could further expand their potential use and result in novel applications. More specifically, the synthesis of composite nanomaterials, including graphenes, CNTs, nanowires, and/or nanoparticles shows great potential for applications, such as gas detection/chemical sensors, electrodes, and/or solar energy harvesting.[8,9]

Recently, the formation of organic–inorganic hybrid nanosystems by the incorporation of metal nanoparticles in or onto the graphitic structures of CNTs or graphene has been reported.[10–12] In particular, noble metal nanoparticles have huge potential in sensing, energy, spectroscopy, and catalysis. For these purposes, silver and gold ions can be reduced to nanoparticle colloids by simple wet chemistry techniques utilizing sodium citrate and sodium borohydride as reducing agents.[13] The size and shape of the nanoparticles can be manipulated by controlling the concentration of reducing agent, capping agents, and seed-mediated growth.[14,15] The controlled growth of nanometer-sized metals is essential to ensure that the unique properties (i.e., plasmon absorption) exhibited by these nanoparticles can be applied to specific applications, such as photovoltaics and catalysis. Plasmonics have recently gained much attention for their ability to improve the absorption characteristics in thin film solar cells.[16] The incorporation of Ag nanoparticles (AgNPs) into an organic solar cell has led to a significant increase in photocurrent and overall power conversion efficiency.[17,18]

Aside from plasmonics, metal nanoparticles find many others applications, especially in catalysis. Although gold complexes have found many uses as homogeneous catalysts for organic transformations, solid gold has long been regarded as a poor catalyst for heterogeneous reactions.[19,20] There is significant evidence, however, that gold nanoclusters deposited on a variety of metal oxide support materials can efficiently catalyze oxidation and reduction reactions as well as carbon–carbon bond formation.[20–22] Size-dependent properties associated with the AuNPs make them an excellent candidate as the active component in a number of catalysts.[23] Taking advantage of these unique properties of

* Address correspondence to exdervishi@ualr.edu, asbiris@ualr.edu.

Received for review October 5, 2011 and accepted December 11, 2011.

Published online December 12, 2011
10.1021/nn203836q

AuNPs could result in increasing their catalytic activity, which is generally slow or difficult to initiate and takes place at higher temperatures.[24,25]

Historically, gold chemistry has received tremendous attention since Hatura's discovery of oxide-supported Au nanocluster catalysts that were used for CO and H_2 oxidation at low temperatures.[26,27] Since then, the investigation of gold-based catalysts has increased drastically.[21,24,25,28] Gold-based catalysts have been used in a range of organic transformations which includes a variety of nucleophilic addition, cascade reactions, C−C bond formation, Fridel-Crafts reaction, C−H bond activation, hydrogenation and dehydrogenation reactions, and oxidation chemistry.[29−34] Furthermore, asymmetric catalysis and total organic synthesis have also been achieved using Au-based catalysts.[35] Highly flexible catalytic systems consisting of carbon supports decorated with AuNPs, have shown significant potential for many reactions including the oxidation of CO for fuel cells, oxidation of diols, and C−C bond formation.[19,36,37] Therefore, synthesizing carbon nanomaterials on an Au catalyst or decorating graphitic nanostructures with AuNPs opens the door to a wide range of new applications for which current technologies are not adequate.

Furthermore, gold has been utilized as a catalyst for carbon nanotube synthesis by many groups around the world.[38−41] Often AuNPs have been mixed with other transition metals to enhance their catalytic potential in the synthesis of nanotubes. For example, various levels of Au doping have been shown to improve the catalytic activity of Ni and lower the reaction temperature for the nanotube formation.[42] Interestingly, in this case, the utilization of pure Au was found to be inactive for the synthesis of CNTs or carbon nanofibers.

Usually, CNT synthesis has been achieved at relatively high temperatures between 850 and 1000 °C. Ong *et al*. demonstrated the growth of CNTs at 1000 °C, on Au catalyst sputtered on amorphous carbon, which was deposited on Si wafers.[43] A high temperature of 1000 °C was required when ethanol was added as the carbon source to this experimental approach. Furthermore, Lin *et al.* synthesized multiwalled carbon nanotubes (MWCNTs) and carbon nanofibers by CVD on Au TEM grid surfaces at 850 °C when utilizing ethylene as the feed gas.[44] It is important to mention that, in this case, only amorphous carbon was reported to be formed at temperatures lower than 750 °C. MWCNTs were also synthesized at temperatures higher than 850 °C on Au films deposited on a Si substrate by electron beam evaporation, utilizing acetylene or other hydrocarbons as a carbon source.[40,45]

Single-walled carbon nanotubes (SWCNTs) were grown on AuNPs at temperatures between 800 and 900 °C, with various feed gases, such as ethanol, ethylene, or methane, and a number of oxides as the catalytic supports.[39,46] The AuNPs were prepared by a block copolymer technique or deposited on different substrates through spin-coating a colloidal solution. Before introducing the hydrocarbon, the catalyst was heat treated or reduced under hydrogen at 800 °C; no SWCNTs were reported to grow at temperatures below 800 °C.[39] Although many groups have reported the growth of CNTs on Au catalysts at relatively high temperatures, Ghorannevis *et al*. synthesized SWCNTs at 750 °C on a thin Au film utilizing ethanol vapors.[38]

Moreover, CNTs (both MW and SWCNTs) were found to grow on metal-free substrates at various temperatures, using different types of hydrocarbons.[47] For example, Takagi *et al*. synthesized SWCNTs over nanodiamond particles at 850 °C using ethanol as a carbon source.[48] The nanodiamond particles separately deposited on two different substrates, graphite or diamond, were found to promote nanotube formation through the "vapor−solid surface−solid" growth mechanism. Interesting findings were reported by Steiner *et al*. about the ability of zirconia nanoparticles to nucleate CNTs at temperatures between 750 and 900 °C, using methane or ethylene as the carbon source.[49] For the first time, it was demonstrated that an oxide can nucleate CNT growth while remaining in an oxidized state. Furthermore, nonmetallic catalysts such as SiC, Al_2O_3, MgO, SiO_x, and other semiconducting substrates have been utilized for nanotube growth, using techniques such as chemical vapor deposition or high temperature and laser annealing.[50−54]

Recently, CNTs or nanowires have been synthesized at very high temperatures (900−1000 °C) with or without the addition of hydrocarbons on graphene oxide or graphite structures (deposited on SiO_2 substrates) coated with various catalytic nanoparticles such as Fe or Ni.[8,55] Hunley *et al*. have reported the synthesis of aligned nanotubes on few-layer graphene sheets deposited on p-type silicon oxide substrates.[55] In this case, a thin film of Ni was used for the formation of catalytically active catalyst particles, and the CNT synthesis was carried out in a CVD furnace with the assistance of Ar and H_2 at 900 °C.[55] Moreover, Cao *et al*. reported the growth of carbon nanowires on graphene oxide coated with $CoCl_2$.[8] A mixture of Ar/H_2 was flown into the set up (with a pressure of 150 Pa) while the temperature was varied between 900 and 1000 °C.

For the first time to our knowledge, we report the catalytic conversion of Au-decorated graphene to nanotubes at relatively low temperatures (500 °C) *without* the need of a hydrocarbon source by utilizing a radio frequency chemical vapor deposition (RF-CVD) reactor. We have previously reported that this technique is very versatile and has been used extensively for the controlled synthesis of high quality CNTs and few-layer graphenes. Some of the advantages are related to the extremely high temperature increase rates that could be responsible for successfully preventing the

metal nanoparticles from migrating over the support surfaces.[56−60] Gold has been previously found to be a challenging catalytic element in the synthesis of CNTs and other carbon nanostructures. The facile method presented in this manuscript provides a methodology for the synthesis of CNTs/graphene composites (without including substrates such as SiO_2) at a low temperature and at atmospheric pressure, utilizing only a carrier gas (noncarbon containing gas). Syntheses on the Au-decorated graphene sheets were also carried out at higher temperatures and in a thermal furnace, for comparison. We foresee that such a finding could make possible the controlled one-step growth of multicomponent organic−inorganic nanosystems with 0, 1, and 2-dimensional morphologies, with applications ranging from solar energy harvesting, supercapacitors, sensing, advanced functional nanocomposites, to nanomedicine.

RESULTS AND DISCUSSION

Prior to its decoration with gold nanoclusters, the commercially available graphene was thoroughly characterized by electron microscopy (both SEM and TEM). Figure 1a and its inset show the SEM images of the unprocessed graphene with lateral size of several micrometers. Figure 1b and its inset are TEM images of the commercially available graphene deposited on the carbon-coated copper grid. Both SEM and TEM analysis revealed the presence of large, transparent graphene sheets with few layers. The thermo-gravimetrical analysis (TGA) of the unprocessed graphene is presented in the Supporting Information (SI). After the gold nanoclusters were deposited on the graphene surfaces, microscopy was performed for the sample characterization. High- and low-magnification SEM images of the decorated graphenes are shown in Figure 1c. After a thorough analysis, it was observed that an average of 40 (±15%) AuNPs were homogeneously deposited on a graphene surface with an area of 350 nm^2. High resolution TEM analyses were used to analyze the diameter distribution of the AuNPs. Figure 1d and the insets present high and low resolution TEM images of the Au-decorated graphene sheets. After analyzing over 100 TEM and SEM images, it was determined that the diameter of the majority of the AuNPs decorating the graphene sheets varied from 6 to12 nm, while a few of them had diameters between 20 and 30 nm. Scanning transmission electron microscopy (STEM) analyses were also performed to further prove the successful decoration of the graphene sheets with AuNPs. The elemental analysis in Figures 1e−h confirms the presence of Au (along with C) on the graphene sheets. For the TEM and STEM studies, the samples were sonicated in order to form a homogeneous solution; however, it was observed that most of the AuNPs were still attached to the graphene surface indicating a strong binding between the two materials.

RF-CVD reactions were carried out under an Ar flow and *without* the addition of any hydrocarbon source, utilizing the functionalized graphene decorated with Au nanoclusters as the catalytic system. Previous studies have clearly indicated that the AuNPs have effective catalytic properties toward CNT nucleation and growth, but the type of substrate affects the reaction kinetics.[39] In our case, the few-layer graphene sheets were found to act as the carbon source, while simultaneously enhancing the catalytic activity of the AuNPs. As a final result, this Au−NP−graphene catalytic system was found to promote CNT growth during the RF-CVD heating. A high-yield catalytic conversion of graphene into CNTs was observed at very low temperatures of only 500 and 600 °C—values that have not previously been reported to sustain any CNT nucleation or growth over an Au-based catalytic system. Figure 2 panels a and b show the SEM images of the CNTs synthesized over the Au-decorated graphene sheets at 500 °C. Moreover, the SEM images in Figure 2 panels c and d indicate a high yield toward the synthesis of random networks of CNTs at 600 °C, *without* the presence of any additional carbon source and only under a mild Ar flow. Figure 2 panels e and f present the TEM images of the CNTs synthesized at 600 °C over the graphene sheets decorated with AuNPs. A thorough TEM analysis indicated the synthesis of a mixture of few- and multiwalled nanotubes with diameters between 10 and 20 nm, which is in excellent agreement with the size of the AuNPs. While most of the Au nanoclusters remained on the graphene surface during its conversion into CNTs, it was observed that a few of the CNTs were found to synthesize between the metal nanoparticles and the graphene, following the tip growth modality.[61] Figure 2 panels g and h and their insets reveal the SEM and TEM images of the CNT/graphene composites after the RF reactions at 650 °C under Ar. The SEM images clearly indicated the presence of tangled tubular structures over the surface of the graphene sheets. This is a very simple method involving a straightforward experimental setup to synthesize CNTs on graphene surfaces at very low temperatures using only a carrier gas and AuNPs as the catalytic agents. As a result, the AuNPs have the ability to convert the 2D structure of graphene into the 1D morphology of nanotubes, by the formation of C−C bonds that are required for the change in the crystalline geometrical structures of the two nanomaterials.

Additionally, RF-driven reactions were performed for the same composite nanosystems, but in the presence of acetylene at similar temperatures: 600 and 650 °C. Electron microscopy analyses were performed to analyze the catalytic conversion of the Au-decorated graphene. Figure 3a−g demonstrate the TEM, SEM, and elemental analyses of the nanotubes synthesized

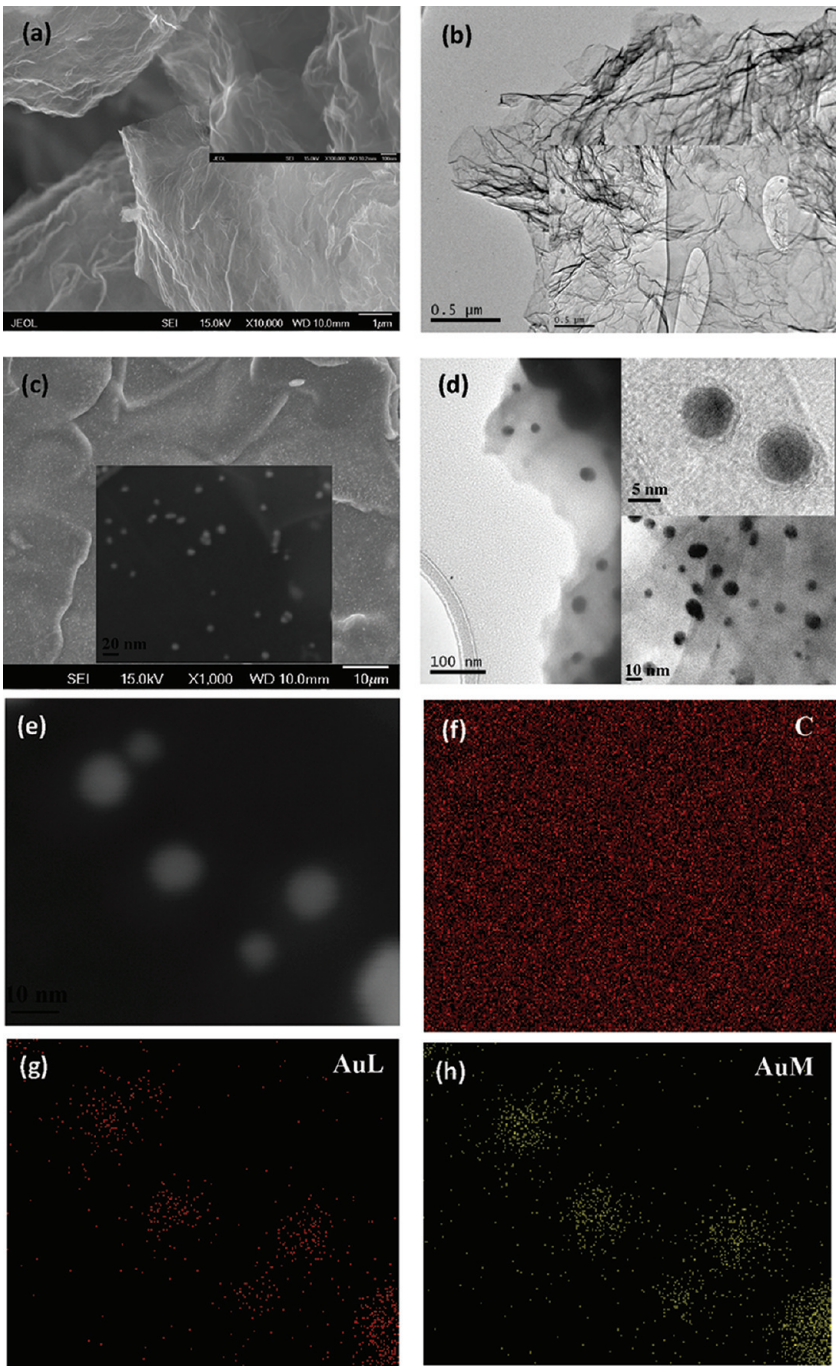

Figure 1. (a, and its inset) SEM images of the unprocessed graphene sheets; (b and its inset) TEM images of the commercially available graphene deposited on the carbon-coated copper grid; (c and its inset) high and low magnification SEM images of the decorated graphene; (d and its insets) high and low resolution TEM images of the Au nanoclusters deposited on the graphene sheets; (e–h) energy dispersive X-ray spectroscopy (EDS) maps indicating the distribution of AuL, AuM, and C, respectively.

on the surface of the functionalized graphene with Au nanoclusters at 600 °C. Figure 3b indicates the presence of long tubular structures with diameters ranging between 15 and 20 nm. The EDS analysis shown in Figure 3d–g, indicates the presence of C, O_2, and Au. As seen in the table of the inset of Figure 3g, Au is only 1.68 wt % compared to C which is 94.13 wt %.

The SEM images in Figure 4a,b demonstrate a high-yield catalytic growth of nanotubes when utilizing acetylene at 650 °C. Furthermore, reactions on the decorated graphene sheets were performed at higher temperatures (>650 °C) with or without a hydrocarbon source and were found to yield similar results (data not shown here). TEM images in Figure 4 indicate the presence of a mixture of few-walled nanotubes and tubular structures with a "bamboo-like" morphology. The formation of such nanostructures has been previously reported by other groups when

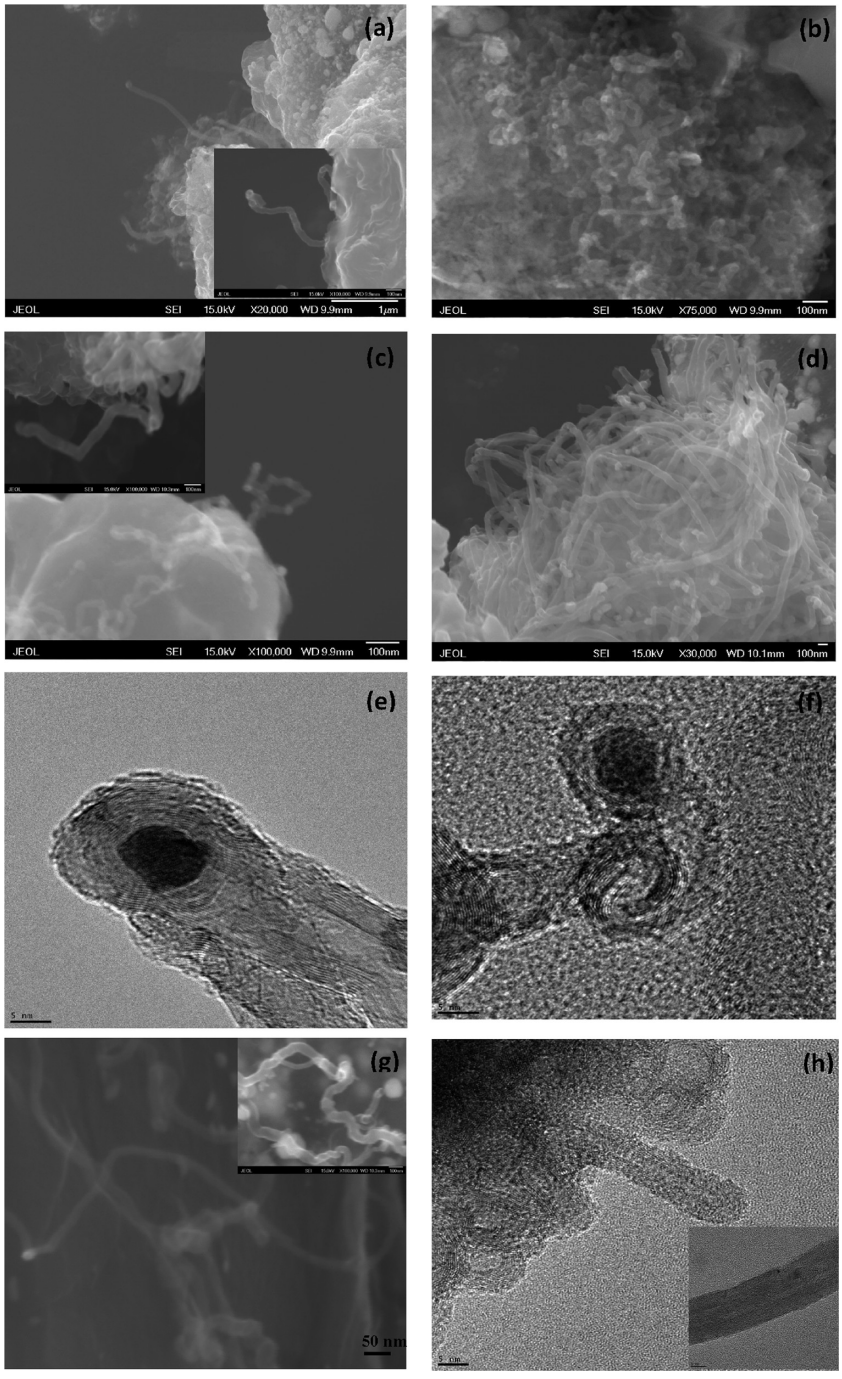

Figure 2. (a and b) SEM images of the CNTs synthesized on the surface of the Au-decorated graphene sheets at 500 °C without the addition of the hydrocarbon feed gas. (c and d) SEM images of the CNTs grown on the Au-decorated graphene sheets at 600 °C under argon. The scale in the inset of panels a and c is 100 nm. (e and f) (scale bar 5 nm) TEM images of the CNTs synthesized from the Au nanoclusters on the functionalized graphene sheets at 600 °C. (g and h, and their insets) SEM and TEM images of the CNT and graphene structures after the RF reactions at 650 °C under Ar. The scale in the insets of panels g and h is 100 and 5 nm, respectively.

utilizing oxide-supported Au nanoclusters for the nucleation and growth of CNTs.[40,44,62] This structural morphology may be correlated with the catalytic properties of the Au nanoclusters and the interactions between the carbon atoms and the Au structures. Sharma *et al*. have also reported that the addition of AuNPs to Ni thin films deposited on SiO_2 substrates has a direct effect on the structural morphology of MWCNTs, resulting in the formation of "herringbone" (cones) and "bamboo"-type structures.[42] Figure 4c presents high and low resolution TEM images of the tubular structures with distinctive morphologies, where the distance between the inner walls (as indicated by the arrows) along the nanotubes was measured to be on average of 18 nm. The high resolution TEM images in Figure 4d–f demonstrate the conversion of the

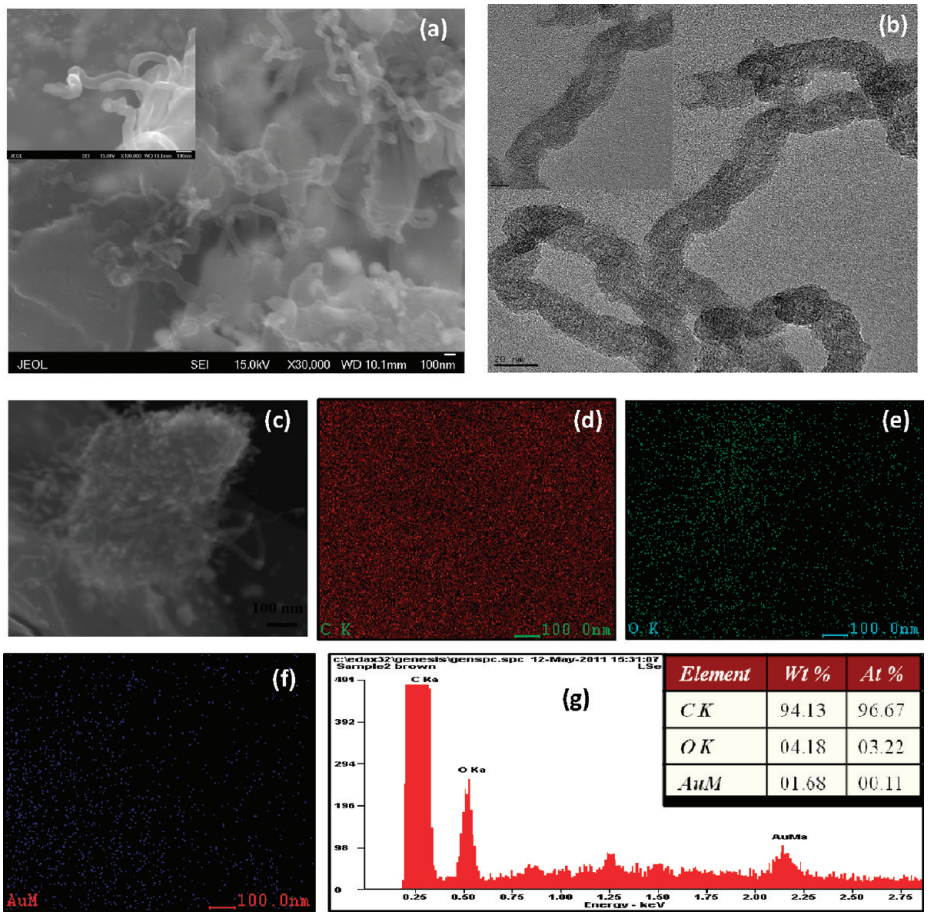

Figure 3. (a and its inset) SEM images of the nanotubes synthesized on the Au-decorated graphene sheets at 600 °C. The scale in the inset of panel a is 100 nm. (b and its inset) TEM images of the tubular structures synthesized at 600 °C utilizing acetylene. The scale in the inset of panel b is 10 nm. (c−g): SEM/EDS analysis indicating the presence of C, O_2, and Au.

graphene sheet into a few-walled CNT. After a detailed study of the TEM images of the AuNPs decorating the graphene sheets, subsequent to the RF treatment, we believe that the first step in the catalytic conversion of graphene is the formation of carbon layers around the Au nanoclusters, which will continue to expand into nanotubes as the reaction progresses. The arrow in Figure 4d indicates the presence of 4 layers on the Au nanoparticle. Ong *et al.* have reported that Au does not dissolve carbon atoms the same way that other metals, such as Co and Fe, do.[43] Carbon diffusion occurs on the surface of the Au nanoclusters.[43] After the carbon atoms solubilize on the surface of the Au nanoclusters, at saturation point, they precipitate out covering the nanocluster surface with graphitic layers as shown in Figure 4d.[39,44] We believe that this process can be explained by two mechanisms: (1) in the absence of carbon source gas, under the thermal excitation, the AuNPs create small defects in the graphitic structure of the graphene layers and through a catalytic reaction process initiate the carbon nanotube formation. During the reaction, graphene decomposes providing a necessary source of carbon for further nanotube growth on the AuNPs; (2) In the presence of a carbon source, the catalytic nanotube growth is further enhanced due to the presence of a higher concentration of the carbon atoms. It may be possible that under these particular reaction conditions, graphene interacts with the AuNPs leading to the formation of nanotubes. Observations such as relatively low reaction temperature, formation of no nanotubes or any other tubular carbonaceous structures in the absence of gold, and evidence of strongly embedded AuNPs into the nanotube structure, have led us to believe that gold plays a major catalytic role in the nanotube growth.

Furthermore, Takagi *et al.* have reported that carbon solubility of Au is extremely low and is dependent upon the size of AuNPs.[63] They reported that, although no CNT growth was observed on large Au nanoclusters (>100 nm), the carbon solubility significantly increased as the size of the AuNPs decreased.[63] Figure 4 panels e and f are TEM images of the same few-walled CNT (taken at different locations) growing out of the graphene edge (as indicated by the circle) with the Au nanoparticle entrapped in its twisted tip. This tip-growth phenomenon (where the nanoparticle is resting on the tip of the tubular carbon structure) has also been reported by others who synthesized CNTs on Au or

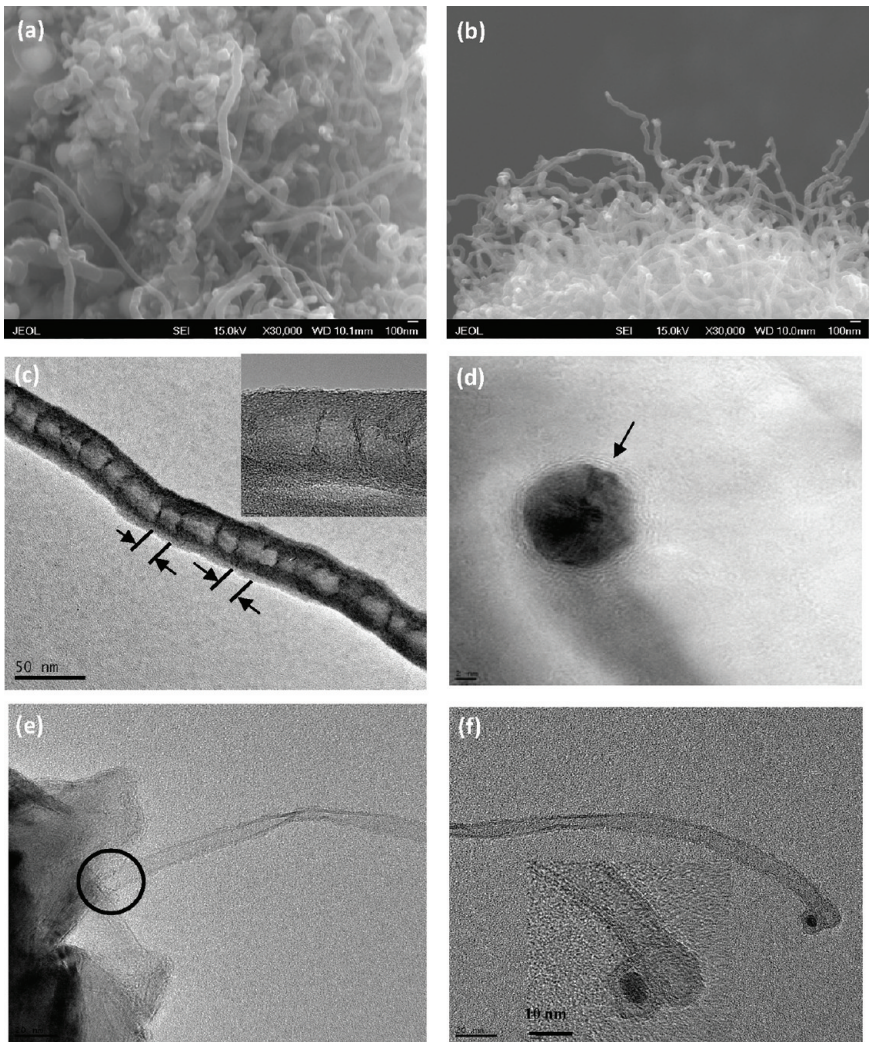

Figure 4. (a and b) SEM images of the synthesized CNTs on the Au-decorated graphene at 650 °C. (c–f and insets) TEM images of the tubular structures and few-walled CNTs synthesized on the graphene sheets utilizing acetylene. The scale in the inset of panel c is 5 nm. (e and f) TEM images of the same nanotube at different locations providing evidence of the "tip-growth" mechanism.

Au-metal alloys.[63] The interaction between the graphene surface and the metal nanoparticle may not have been very strong, since the catalyst nanoparticle was lifted from the graphene surface. A similar tip-growth mechanism has been reported to influence the alignment of nanotubes grown on the Ni-decorated graphene.[55] We are currently performing more studies in our laboratories to further understand the growth mechanism of CNTs on the graphene-decorated sheets.

Reactions were also performed in a TGA furnace under Ar, following the same conditions as the ones in the RF generator. The unprocessed graphene and the functionalized graphene decorated with AuNPs were separately heated at various temperatures (600, 650, and 700 °C) for 30 min and then cooled to room temperature. Figure 5 presents the mass loss curve of the commercial graphene and the Au-decorated graphene heated to 600 °C under Ar. The TGA curve indicated that the weight of the unprocessed graphene decreases from 100% to about 62% indicating a mass loss of 38%.

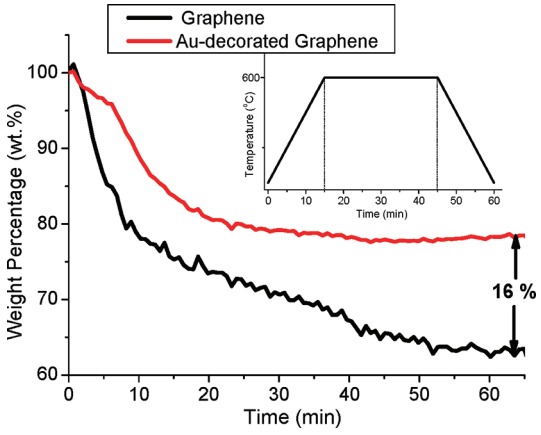

Figure 5. The TGA curve of the commercial graphene and the Au-decorated graphene heated to 600 °C under Ar, respectively. The inset presents the temperature *versus* time set up for every experiment in the TGA furnace.

This mass loss is explained based on the graphene becoming thermally unstable as the temperature increases.

The inset in Figure 5 presents the temperature *versus* time setup for every experiment performed in the TGA furnace. It was determined that the Au-decorated graphene loses about 22% of its mass at 600 °C and 26% at 650 °C (not shown here) and 700 °C (Figure S3 in the SI section). The mass loss percentage during the thermal decomposition process is smaller than the one for the commercial graphene under identical conditions. This 16% mass loss difference at 600 °C is believed to be due to the Au-catalyzed conversion of graphene into CNTs.

Microscopy analyses of the TGA-generated samples revealed a very low-yield conversion of decorated graphene compared to the reactions performed under the RF generator, explained by the possible RF excitation of the AuNPs that could affect their ability to interact with the carbon atoms. The presence of the electromagnetic RF fields, of a 350 kHz frequency, is believed to be responsible for a better catalytic conversion of the carbon atoms into graphitic structures, with an enhanced quality and efficiency. We have previously seen differences in the morphological properties of the nanotubes, such as diameter and crystallinity, when synthesized in a conventional thermal furnace or in the RF generator.[64,65] Nonetheless, it is important to affirm that the catalytic conversion occurs under different heating methods (inductive or resistive thermal heating). We are currently investigating this phenomenon to further understand the growth mechanism of CNTs in the electrical furnace and the RF generator.

RF reactions were performed on the nonfunctionalized graphene with and without acetylene at 600 and 650 °C. It is important to mention that, after thorough SEM analyses, no CNT growth was detected at various temperatures. SEM images are shown in Supporting Information Figures S4a and b. This has also been reported by others, where nonfunctionalized graphene sheets containing no nanoparticles or other impurities failed to yield CNT or other carbon nanostructure growth.[66] Therefore, we believe that the conversion of the graphene into the CNTs at various temperatures occurs only in the presence of a catalyst nanoparticle, which in this case is Au. Next, hydrogen was used to reduce the Au nanoclusters, and reactions were carried out at 600 °C with and without the addition of the hydrocarbon. Figure S5 panels a and b in the Supporting Information show the low and high magnification SEM images of the nanotubes synthesized on the decorated graphene structures under Ar. Moreover, Figure S5 panels c and d illustrate the SEM images of a high-yield growth of the tubular nanostructures on the graphene structures utilizing acetylene. It was observed that, in both reactions, the nanotubes are decorated with nanoparticles (as indicated by arrows). This phenomenon was also observed by Zhang *et al.* on Au-coated silicon substrates at 850 °C.[45] The nanoparticles or other impurities attached to the outer surface of the nanotubes can be removed by the addition of water vapor in the CVD set up.[45]

Synthesis reactions in identical conditions were performed on SiO_2 wafers coated with Au nanoclusters at 600 and 650 °C under Ar with and without addition of the feed gas. Figure S6 in the Supporting Information presents the SEM images of the RF-treated SiO_2 substrates. Electron microscopy did not indicate the presence of any CNTs on the surface of the Au-coated SiO_2 wafers with or without hydrocarbon source at various temperatures, indicating that the graphene substrate is necessary for the CNT synthesis under these particular reaction conditions. This indicates that the carbon source for the CNT synthesis initiates only from the graphene sheets as previously reported by others.[55]

CONCLUSIONS

We have clearly demonstrated, for the first time to our best knowledge, that graphene structures play a major role in the catalytic activity of AuNPs and that they can be responsible for the catalytic formation of CNTs. It is believed that graphene can be converted into tubular nanotube-like structures without the need of any additional carbon source, but only in the presence of the AuNPs. Moreover, the catalytic reaction temperature (500 °C) was found to be lower than any other similar value reported in the literature, indicating that graphene could lower the CNT synthesis temperature, when used as a catalytic support material. In addition, under the same reaction conditions, SiO_2 substrates coated with AuNPs were found to produce no CNTs or other tubular structures at any temperature. We are currently performing additional studies, using other metal nanomaterials in a similar morphology, to assess their ability to produce catalytically various types of carbonaceous structures. Such findings could be the foundation for new technologies used in a number of applications, ranging from capacitors, fuel cell membranes, and solar energy, to nanobiomedicine. These applications could be further improved by using this newly described multicomponent system formed of nanomaterials with 0, 1, and 2-dimensional morphologies.

MATERIALS AND METHODS

Graphenes with diameters of approximately 10 μm and an average thickness of less than 1 nm were purchased from Ångstron Materials, Inc. The graphene was first functionalized and then decorated with gold nanoclusters *via* chemical treatment. Carboxylic-functionalized graphene was prepared as previously described by Kim *et al.*[67] Specifically, graphene was mixed with sulfuric and nitric acid (3:1 ratio) and stirred

overnight. Next, the solution was filtered and continuously washed with DI water until the pH was neutral and dried overnight in the oven at 80 °C.

The functionalized graphene with carboxylic groups was then decorated with gold nanoclusters *via* citrate reduction of Au(III).[11,14] Specifically, 75 mg of functionalized graphene was added to 275 mL of 18 MΩ water and dispersed by sonication for 2 h. A 250 mL sample of 0.51 mM $HAuCl_4$ in 18 MΩ water was added to the graphene dispersion and stirred for 30 min to promote a uniform mixing. The reaction mixture was heated to 80 °C after which 10 mL of 0.88 M sodium citrate was added dropwise. Figure S1 in the Supporting Information shows a schematic of the reaction set up used for the decoration of graphene with Au nanoclusters. The reaction was allowed to proceed for 1 h at this temperature and then stirred overnight in ambient conditions. Purification of the Au-decorated graphene was accomplished by centrifugation, decanting the supernatant, and washing with 18 MΩ water three successive times.

The catalytic conversion of Au-decorated graphene into CNTs was accomplished utilizing RF-CVD and thermal decomposition techniques for comparative purposes. For each reaction, a small amount of about 10 mg of the Au-decorated graphene was finely spread on a susceptor, which was placed inside a quartz tube resting at the center of the RF generator coil with a frequency of 350 kHz.[59] First, the quartz tube was flushed with argon used as a carrier gas flowing at 150 mL/min for 10 min. Once the graphene boat reached the target temperature, acetylene was added at 5 mL/min for 30 min. Subsequently, the hydrocarbon source and the generator were turned off, and the sample was allowed to cool to room temperature under argon flow for 10 min. The reactions were carried out at the following temperatures: 500, 600, 650, and 700 °C. Separate reactions were carried out without the hydrocarbon source by only using argon at target temperatures for 30 min and then samples were cooled to room temperature. Similar experiments were performed using the unprocessed graphene with and without the addition of hydrocarbon. Next, a control gold solution was prepared in a similar manner without the addition of graphene. The latter was deposited on Si wafers with SiO_2 native layer and reactions were performed in the RF generator under conditions identical to the ones performed with the Au-decorated graphene.

Thermo-gravimetrical analyses were performed by heating the sample under argon (the Au-decorated and the nondecorated graphene) from 25 °C to the target temperature following the same conditions as in the RF-CVD technique. The resulting samples were characterized by various techniques and compared with the ones synthesized in RF-CVD.

Acknowledgment. The financial support from the Arkansas Science & Technology Authority (Grant No. 08-CAT-03), the Department of Energy (DE-FG36-06GO86072), and National Science Foundation (NSF/EPS-1003970) is greatly appreciated. The editorial assistance of Dr. M. Ringer is also acknowledged.

Supporting Information Available: Details on the characterization techniques; thermo-gravimetrical analysis of unprocessed and Au-decorated graphene; SEM images of the pristine and Au-decorated graphene after the RF treatment; SEM images of the Au-coated SiO_2 wafers after exposed to RF generator. This material is available free of charge *via* the Internet at http://pubs.acs.org.

REFERENCES AND NOTES

1. Iijima, S. Helical Microtubules of Graphitic Carbon. *Nature* **1991**, *6348*, 56–58.
2. Novoselov, K. S.; Geim, A. K.; Morozov, S. V.; Jiang, D.; Katsnelson, M. I.; Grigorieva, I. V.; Dubonos, S. V.; Firsov, A. A. Two-Dimensional Gas of Massless Dirac Fermions in Graphene. *Nature* **2005**, *7065*, 197–200.
3. Schedin, F.; Geim, A. K.; Morozov, S. V.; Hill, E. W.; Blake, P.; Katsnelson, M. I.; Novoselov, K. S. Detection of Individual Gas Molecules Adsorbed on Graphene. *Nat. Mater.* **2007**, *9*, 652–655.
4. Jung, I.; Dikin, D. A.; Piner, R. D.; Ruoff, R. S. Tunable Electrical Conductivity of Individual Graphene Oxide Sheets Reduced at "Low" Temperatures. *Nano Lett.* **2008**, *12*, 4283–4287.
5. Wang, X.; Zhi, L.; Mullen, K. Transparent, Conductive Graphene Electrodes for Dye-Sensitized Solar Cells. *Nano Lett.* **2008**, *1*, 323–327.
6. Rangel, N. L.; Seminario, J. M. Vibronics and Plasmonics Based Graphene Sensors. *J. Chem. Phys.* **2010**, *12*, 125102.
7. Merchant, C. A.; Healy, K.; Wanunu, M.; Ray, V.; Peterman, N.; Bartel, J.; Fischbein, M. D.; Venta, K.; Luo, Z.; Johnson, A. T.; *et al.* DNA Translocation Through Graphene Nanopores. *Nano Lett.* **2010**, *8*, 2915–2921.
8. Cao, X.; He, Q.; Shi, W.; Li, B.; Zeng, Z.; Shi, Y.; Yan, Q.; Zhang, H. Graphene Oxide as a Carbon Source for Controlled Growth of Carbon Nanowires. *Small* **2011**, *6*, 1199–1202.
9. Bai, H.; Li, C.; Shi, G. Functional Composite Materials Based on Chemically Converted Graphene. *Adv. Mater.* **2011**, *3*, 1089–1115.
10. Muszynski, R.; Seger, B.; Kamat, P. V. Decorating Graphene Sheets with Gold Nanoparticles. *J. Phys. Chem. C* **2008**, *14*, 5263–5266.
11. Goncalves, G.; Marques, P. A. A. P.; Granadeiro, C. M.; Nogueira, H. I. S.; Singh, M. K.; Grácio, J. Surface Modification of Graphene Nanosheets with Gold Nanoparticles: The Role of Oxygen Moeties at the Graphene Surface on Gold Nucleation and Growth. *Chem. Mater.* **2009**, *20*, 4796–4802.
12. Lu, J.; Do, I.; Drzal, L. T.; Worden, R. M.; Lee, I. Nanometal-Decorated Exfoliated Graphite Nanoplatelet Based Glucose Biosensors with High Sensitivity and Fast Response. *ACS Nano* **2008**, *9*, 1825–1832.
13. Lee, P. C.; Meisel, D. Adsorption and Surface-Enhanced Raman of Dyes on Silver and Gold Sols. *J. Phys. Chem.* **1982**, *17*, 3391–3395.
14. Kumar, S.; Gandhi, K. S.; Kumar, R. Modeling of Formation of Gold Nanoparticles by Citrate Method. *Ind. Eng. Chem. Res.* **2007**, *10*, 3128–3136.
15. Nikoobakht, B.; El-Sayed, M. A. Preparation and Growth Mechanism of Gold Nanorods (NRs) Using Seed-Mediated Growth Method. *Chem. Mater.* **2003**, *10*, 1957–1962.
16. Atwater, H. A.; Polman, A. Plasmonics for Improved Photovoltaic Devices. *Nat. Mater.* **2010**, *3*, 205–213.
17. Yoon, W.; Jung, K.; Liu, J.; Duraisamy, T.; Revur, R.; Teixeira, F. L.; Sengupta, S.; Berger, P. R. Plasmon Enhanced Optical Absorption and Photocurrent in Organic Bulk Heterojunction Photovoltaic Devices Using Self-Assembled Layer of Silver Nanoparticles. *Solar Energy Mater. Solar Cells* **2010**, *2*, 128–132.
18. Kim, S.; Na, S.; Jo, J.; Kim, D.; Nah, Y. Plasmon Enhanced Performance of Organic Solar Cells Using Electrodeposited Ag Nanoparticles. *Appl. Phys. Lett.* **2008**, *7*, 073307–3.
19. Thompson, D. New Advances in Gold Catalysis Part I. *Gold Bulletin* **1998**, *4*, 111–118.
20. Ueda, A.; Haruta, M. Nitric Oxide Reduction with Hydrogen, Carbon Monoxide, and Hydrocarbons over Gold Catalysts. *Gold Bull.* **1999**, *1*, 3–11.
21. Li, Z.; Brouwer, C.; He, C. Gold-Catalyzed Organic Transformations. *Chem. Rev.* **2008**, *8*, 3239–3265.
22. Tsunoyama, H.; Sakurai, H.; Ichikuni, N.; Negishi, Y.; Tsukuda, T. Colloidal Gold Nanoparticles as Catalyst for Carbon–Carbon Bond Formation: Application to Aerobic Homocoupling of Phenylboronic Acid in Water. *Langmuir* **2004**, *26*, 11293–11296.
23. Shapiro, N. D.; Toste, F. D. A Reactivity-Driven Approach to the Discovery and Development of Gold-Catalyzed Organic Reactions. *Synlett* **2010**, *5*, 675–691.
24. Arcadi, A. Alternative Synthetic Methods through New Developments in Catalysis by Gold. *Chem. Rev.* **2008**, *8*, 3266–3325.
25. Gorin, D. J.; Sherry, B. D.; Toste, F. D. Ligand Effects in Homogenous Au Catalysis. *Chem. Rev.* **2008**, *8*, 3351–3378.
26. Haruta, M.; Yamada, N.; Kobayashi, T.; Iijima, S. Gold Catalysts Prepared by Coprecipitation for Low-Temperature Oxidation of Hydrogen and of Carbon Monoxide. *J. Catal.* **1989**, *2*, 301–309.

27. Haruta, M.; Kobayashi, T.; Sano, H.; Yamada, N. Novel Gold Catalysts for the Oxidation of Carbon-Monoxide at Low Temperature. *Chem. Lett.* **1987**, *2*, 405–408.
28. Sardar, R.; Funston, A. M.; Mulvaney, P.; Murray, R. W. Gold Nanoparticles: Past, Present and Future. *Langmuir* **2009**, *24*, 13840–13851.
29. Stephen, A.; Hashmi, P. D. K.; Schwarz, D. C. L.; Choi, J. H.; Frost, T. M. A New Gold-Catalyzed C−C Bond Formation. *Angew. Chem., Int. Ed.* **2000**, *39*, 2285–2288.
30. Fructos, M. R.; Belderrain, T. R.; De Frémont, P.; Scott, N. M.; Nolan, S. P.; Díaz-Requejo, M. M.; Pérez, P. J. Gold Catalyst for Carbene Transfer Reactions from Ethyl Diazoacetate. *Angew. Chem., Int. Ed.* **2005**, *33*, 5284–5288.
31. Sromek, A. W.; Rubina, M.; Gevorgyan, V. 1,2-Halogen Migration in Haloallenyl Ketones: Regiodivergent Synthesis of Halofurans. *J. Am. Chem. Soc.* **2005**, *127*, 10500–10501.
32. Lian, J.; Chen, P.; Lin, Y.; Ting, H.; Liu, R. Gold-Catalyzed Intramolecular [3 + 2]-Cycloaddition of Arenyne-Yne Functionalities. *J. Am. Chem. Soc.* **2006**, *35*, 11372–11373.
33. Schwier, T.; Sromek, A. W.; Yap, D. M. L.; Chernyak, D.; Gevorgyan, V. Mechanistically Diverse Copper-, Silver- and Gold-Catalyzed Acyloxy and Phosphatyloxy Migrations: Efficient Synthesis of Heterocycles *via* Cascade Migration/Cycloisomerization Approach. *J. Am. Chem. Soc.* **2007**, *129*, 9868–9878.
34. Li, Z.; Capretto, D. A.; Rahaman, R. O.; He, C. Gold(III)-Catalyzed Nitrene Insertion into Aromatic and Benzylic C−H Groups. *J. Am. Chem. Soc.* **2007**, *40*, 12058–12059.
35. Trost, B. M.; Dong, G. Total Synthesis of Bryostatin 16 Using Atom-Economical and Chemoselective Approaches. *Nature* **2008**, *7221*, 485–488.
36. Prati, L.; Rossi, M. Gold on Carbon as a New Catalyst for Selective Liquid Phase Oxidation of Diols. *J. Catal.* **1998**, *2*, 552–560.
37. Kim, W. B.; Voitl, T.; Rodriguez-Rivera, G. J.; Dumesic, J. A. Powering Fuel Cells with CO *via* Aqueous Polyoxometalates and Gold Catalysts. *Science* **2004**, *5688*, 1280–1283.
38. Ghorannevis, Z.; Kato, T.; Kaneko, T.; Hatakeyama, R. Effect of Gold Catalytic Layer Thickness on Growth of Single-Walled Carbon Nanotubes Using Thermal and Plasma CVD. *J. Plasma Fusion Res. Ser.* **2009**, *8*, 595–598.
39. Bhaviripudi, S.; Mile, E.; Steiner, S. A.; Zare, A. T.; Dresselhaus, M. S.; Belcher, A. M.; Kong, J. CVD Synthesis of Single-Walled Carbon Nanotubes from Gold Nanoparticle Catalysts. *J. Am. Chem. Soc.* **2007**, *6*, 1516–1517.
40. Luo, C.; Liu, L.; Jiang, K.; Zhang, L.; Li, Q.; Fan, S. Growth Mechanism of Y-Junctions and Related Carbon Nanotube Junctions Synthesized by Au-Catalyzed Chemical Vapor Deposition. *Carbon* **2008**, *3*, 440–444.
41. Tominaga, M.; Ohira, A.; Kubo, A.; Taniguchi, I.; Kunitake, M. Growth of Carbon Nanotubes on a Gold (111) Surface Using Two-Dimensional Iron Oxide Nanoparticle Catalysts Derived from Iron Storage Protein. *Chem. Commun. (Cambridge)* **2004**, *13*, 1518–1519.
42. Sharma, R.; Chee, S. W.; Herzing, A.; Miranda, R.; Rez, P. Evaluation of the Role of Au in Improving Catalytic Activity of Ni Nanoparticles for the Formation of One-Dimensional Carbon Nanostructures. *Nano Lett.* **2011**, *6*, 2464–71.
43. Ong, S. E.; Zhang, S.; Hsieh, J. H.; Du, H.; Oh, S. H. Growth of Carbon Nanotubes *via* Rapid Thermal Processing from Sputtered Amorphous Carbon. *Int. J. Nanomanuf.* **2008**, *2*, 40–49.
44. Lin, J. H.; Chen, C. S.; Rummeli, M. H.; Zeng, Z. Y. Self-Assembly Formation of Multiwalled Carbon Nanotubes on Gold Surfaces. *Nanoscale* **2010**, *2*, 2835–2840.
45. Zhang, Y.; Li, R.; Liu, H.; Sun, X.; Mérel, P.; Désilets, S. Integration and Characterization of Aligned Carbon Nanotubes on Metal/Silicon Substrates and Effects of Water. *Appl. Surf. Sci.* **2009**, *9*, 5003–5008.
46. Takagi, D.; Homma, Y.; Hibino, H.; Suzuki, S.; Kobayashi, Y. Single-Walled Carbon Nanotube Growth from Highly Activated Metal Nanoparticles. *Nano Lett.* **2006**, *12*, 2642–2645.
47. Kumar, M.; Ando, Y. Chemical Vapor Deposition of Carbon Nanotubes: A Review on Growth Mechanism and Mass Production. *J. Nanosci. Nanotechnol.* **2010**, *10*, 3739–3758.
48. Takagi, D.; Kobayashi, Y.; Homma, Y. Carbon Nanotube Growth from Diamond. *J. Am. Chem. Soc.* **2009**, *131*, 6922–6923.
49. Steiner, S. A., III; Baumann, T. F.; Bayer, B. C.; Blume, R.; Worsley, M. A.; Moberly-Chan, W. J.; Shaw, E. L.; Schloegl, R.; Hart, A. J.; Hofmann, S.; *et al*. Nanoscale Zirconia as a Nonmetallic Catalyst for Graphitization of Carbon and Growth of Single- and Multiwall Carbon Nanotubes. *J. Am. Chem. Soc.* **2009**, *131*, 12144–12154.
50. Botti, S.; Ciardi, R.; Asilyan, L.; De Dominicis, L.; Fabbri, F.; Orlanducci, S.; Fiori, A. Carbon Nanotubes Grown by Laser-Annealing of SiC Nanoparticles. *Chem. Phys. Lett.* **2004**, *400*, 264–267.
51. Rummeli, M. H.; Bachmatiuk, A.; Börrnert, F.; Schäffel, F.; Ibrahim, I.; Cendrowski, K.; Simha-Martynkova, G.; Plachá, D.; Borowiak-Palen, E.; Cuniberti, G.; *et al*. Synthesis of Carbon Nanotubes with and without Catalyst Particles. *Nanoscale Res. Lett.* **2011**, *6*, 303–312.
52. Kusunoki, M.; Rokkaku, M.; Suzuki, T. Epitaxial Carbon Nanotube Film Self Organized by Sublimation Decomposition of Silicon Carbide. *Appl. Phys. Lett.* **1997**, *71*, 2620–2622.
53. Liu, H.; Takagi, D.; Ohno, H.; Chiashi, S.; Chokan, T.; Homma, Y. Growth of Single-Walled Carbon Nanotubes from Ceramic Particles by Alcohol Chemical Vapor Deposition. *Appl. Phys. Express* **2008**, *1*, 014001.
54. Liu, B.; Tang, D. M.; Sun, C.; Liu, C.; Ren, W.; Li, F.; Yu, W. J.; Yin, L. C.; Zhang, L.; Jiang, C.; *et al*. Importance of Oxygen in the Metal-Free Catalytic Growth of Single-Walled Carbon Nanotubes from SiOx by a Vapor−Solid−Solid Mechanism. *J. Am. Chem. Soc.* **2011**, *133*, 197–199.
55. Hunley, D. P.; Johnson, S. L.; Stieha, J. K.; Sundararajan, A.; Meacham, A. T.; Ivanov, I. N.; Strachan, D. R. Crystallographically Aligned Carbon Nanotubes Grown on Few-Layer Graphene Films. *ACS Nano* **2011**, *5*, 6403–6409.
56. Dervishi, E.; Li, Z.; Watanabe, F.; Saini, V.; Biris, A. R.; Xu, Y.; Biris, A. S. High Aspect Ratio and Horizontally Oriented Carbon Nanotubes Grown by RF-cCVD on Si Substrates. *Diamond Relat. Mater.* **2010**, *1*, 67–72.
57. Biris, A. R.; Lupu, D.; Gruneis, A.; Ayala, P.; Rummeli, M. H.; Pichler, T.; Li, Z.; Xu, Y.; Misan, I.; Dervishi, E.; *et al*. High-Quality Double-Walled Carbon Nanotubes Grown by a Cold-Walled Radio Frequency Chemical Vapor Deposition Process. *Chem. Mater.* **2008**, *10*, 3466–3472.
58. Dervishi, E.; Li, Z.; Shyaka, J.; Watanabe, F.; Biswas, A.; Umwungeri, J. L.; Courte, A.; Biris, A. R.; Kebdani, O.; Biris, A. S. The Role of Hydrocarbon Concentration on the Synthesis of Large Area Few to Multilayer Graphene Structures. *Chem. Phys. Lett.* **2011**, *4−6*, 390–395.
59. Dervishi, E.; Li, Z.; Watanabe, F.; Courte, A.; Biswas, A.; Biris, A. R.; Saini, V.; Xu, Y.; Biris, A. S. Versatile Catalytic System for the Large-Scale and Controlled Synthesis of Single-Wall, Double-Wall, Multiwall, and Graphene Carbon Nanostructures. *Chem. Mater.* **2009**, *22*, 5491–5498.
60. Dervishi, E.; Li, Z.; Watanabe, F.; Biswas, A.; Xu, Y.; Biris, A. R.; Saini, V.; Biris, A. S. Large Scale Graphene Production by RF-cCVD Method. *Chem. Comm* **2009**, *27*, 4061–4063.
61. Dervishi, E.; Li, Z.; Xu, Y.; Saini, V.; Biris, A. R.; Lupu, D.; Biris, A. S. Carbon Nanotubes: Synthesis, Properties, and Applications. *Part. Sci. Technol.* **2009**, *2*, 107–125.
62. Lee, S.; Yamada, M.; Miyake, M. Synthesis of Carbon Nanotubes over Gold Nanoparticle Supported Catalysts. *Carbon* **2005**, *13*, 2654–2663.
63. Takagi, D.; Kobayashi, Y.; Hibino, H.; Suzuki, S.; Homma, Y. Mechanism of Gold-Catalyzed Carbon Material Growth. *Nano Lett.* **2008**, *3*, 832–835.
64. Little, R.; Biris, A. R.; Lupu, D.; Xu, Y.; Li, Z.; Dervishi, E.; Biris, A. S. On the Dynamical Ferromagnetic, Quantum Hall, and Relativistic Effects on the Carbon Nanotubes Nucleation and Growth Mechanism. *J Magn. Magn. Mater.* **2008**, *3−4*, 540–547.
65. Biris, A. R.; Biris, A. S.; Lupu, D.; Trigwell, S.; Dervishi, E.; Rahman, Z.; Marginean, P. Catalyst Excitation by Radio Frequency for Improved Carbon Nanotubes Synthesis. *Chem. Phys. Lett.* **2006**, *1−3*, 204–208.

66. Lin, J. H.; Chen, C. S.; Rummeli, M. H.; Bachmatiuk, A.; Zeng, Z. Y.; Ma, H. L.; Buchner, B.; Chen, H. W. Growth of Carbon Nanotubes Catalyzed by Defect-Rich Graphite Surfaces. *Chem. Mater.* **2011**, *7*, 1637–1639.
67. Kim, T.; Kim, H. Effect of Acid-Treated Carbon Nanotube and Amine-Terminated Polydimethylsiloxane on the Rheological Properties of Polydimethylsiloxane/Carbon Nanotube Composite System. *Korea-Aust. Rheol. J.* **2010**, *22*, 205–210.